Acta Oncologica, 2013; 52: 604–611

informa
healthcare

ORIGINAL ARTICLE

Dynamic contrast-enhanced magnetic resonance imaging of the metastatic potential of tumors: A preclinical study of cervical carcinoma and melanoma xenografts

KIRSTI MARIE ØVREBØ, CHRISTINE ELLINGSEN, TORD HOMPLAND & EINAR K. ROFSTAD

Group of Radiation Biology and Tumor Physiology, Department of Radiation Biology, Institute for Cancer Research, Oslo University Hospital, Oslo, Norway.

Abstract

Background. Gadolinium diethylene-triamine penta-acetic acid (Gd-DTPA)-based dynamic contrast-enhanced magnetic resonance imaging (DCE-MRI) has been suggested to be a useful non-invasive method for providing biomarkers for personalized cancer treatment. In this preclinical study, we investigated whether Gd-DTPA-based DCE-MRI may have the potential to differentiate between poorly and highly metastatic tumors. *Material and methods.* CK-160 cervical carcinoma and V-27 melanoma xenografts were used as tumor models. Fifty-six tumors were imaged, and parametric images of K^{trans} (the volume transfer constant of Gd-DTPA) and v_e (the fractional distribution volume of Gd-DTPA) were produced by pharmacokinetic analysis of the DCE-MRI series. The host mice were examined for lymph node metastases immediately after the DCE-MRI. *Results.* Highly metastatic tumors showed lower values for median K^{trans} than poorly metastatic tumors ($p = 0.00033$, CK-160; $p < 0.00001$, V-27). Median v_e was lower for highly than for poorly metastatic V-27 tumors ($p = 0.047$), but did not differ significantly between metastatic and non-metastatic CK-160 tumors ($p > 0.05$). *Conclusion.* This study supports the clinical attempts to establish DCE-MRI as a method for providing biomarkers for tumor aggressiveness and suggests that tumors showing low K^{trans} and low v_e values may have high probability of lymphogenous metastatic dissemination.

Dynamic contrast-enhanced magnetic resonance imaging (DCE-MRI) is used routinely to provide anatomical information on tumors and surrounding normal tissues. The uptake and retention of low-molecular-weight contrast agents in tumors is determined primarily by the blood perfusion, the vessel wall permeability, and the size of the extravascular, extracellular space [1]. Parametric images of K^{trans} (the volume transfer constant of the contrast agent), v_e (the fractional distribution volume of the contrast agent), and parameters related to K^{trans} and v_e can be produced by pharmacokinetic analysis of DCE-MRI data [2]. Investigations of several histological types of cancer have shown weak but statistically significant correlations between parametric MR images and established prognostic factors or outcome of radiation therapy [3]. These findings have led to the suggestion that DCE-MRI may provide biomarkers for personalized cancer treatment [4].

The potential of DCE-MRI-derived parametric images as biomarkers for personalized cancer treatment is currently being evaluated in our laboratory by using human tumor xenografts as preclinical models of cancer. Gadolinium diethylene-triamine penta-acetic acid (Gd-DTPA) is used as contrast agent in most of these studies. The studies carried out thus far have suggested that K^{trans} and/or v_e may provide valuable information on the blood perfusion, the extent of hypoxia, and the radioresponsiveness of tumors [5–9]. Tumors showing low K^{trans} values in combination with low v_e values have been found to be resistant to radiation therapy and to have high fractions of radiation resistant hypoxic cells [8,9]. The possibility that DCE-MRI may provide

Correspondence: E. K. Rofstad, Department of Radiation Biology, Institute for Cancer Research, Norwegian Radium Hospital, Box 4953 Nydalen, 0424 Oslo, Norway. Tel: +47 22781206. Fax: +47 22781207. E-mail: einar.k.rofstad@rr-research.no

(Received 3 December 2011; accepted 24 April 2012)

ISSN 0284-186X print/ISSN 1651-226X online
DOI: 10.3109/0284186X.2012.689851

information on the metastatic potential of tumors was investigated in the present work. Experimental and clinical studies have suggested that tumor hypoxia may promote metastatic spread [10], so we hypothesized that highly metastatic tumors would be characterized by low values of K^{trans} and/or v_e. To test this hypothesis, CK-160 cervical carcinoma and V-27 melanoma xenografts were subjected to DCE-MRI and, immediately afterwards, the host mice were euthanized and examined for lymph node metastases.

Material and methods

Tumor models

CK-160 cervical carcinoma and V-27 melanoma xenografts growing in adult female BALB/c *nu/nu* mice were used as tumor models [11,12]. Tumors were initiated from cells cultured in RPMI-1640 medium supplemented with 13% bovine calf serum, 250 mg/l penicillin, and 50 mg/l streptomycin. Approximately 5.0×10^5 cells in 10 µl of Hanks' balanced salt solution were inoculated intramuscularly in the leg. Twenty-one mice with CK-160 tumors and 35 mice with V-27 tumors were included in the study. The DCE-MRI was carried out with mice anesthetized with fentanyl citrate, fluanisone, and midazolam in doses of 0.63 mg/kg, 20 mg/kg, and 10 mg/kg, respectively. Animal care and experimental procedures were in accordance with the Interdisciplinary Principles and Guidelines for the Use of Animals in Research, Marketing, and Education (New York Academy of Sciences, New York, NY, USA).

DCE-MRI

DCE-MRI was carried out as described earlier [6–9]. Briefly, Gd-DTPA (Schering, Berlin, Germany) was administered in a bolus dose of 0.3 mmol/kg. T_1-weighted images (TR = 200 ms, TE = 3.2 ms, and $\alpha_{T1} = 80°$) were recorded at a spatial resolution of $0.31 \times 0.31 \times 2.0$ mm^3 and a time resolution of 14 s by using a 1.5-T whole-body scanner (Signa; General Electric, Milwaukee, WI, USA) and a slotted tube resonator transceiver coil constructed for mice. The coil was insulated with styrofoam to prevent excessive heat loss from the mice. The body core temperature of the mice was kept at 37–38°C during imaging by using a thermostatically regulated heating pad. Two calibration tubes, one with 0.5 mmol/l Gd-DTPA in 0.9% saline and the other with 0.9% saline only, were placed adjacent to the mice in the coil. The tumors were imaged axially in a single section through the tumor center. Sagittal scans were used to localize the tumor and determine the position of the axial scan. The number of voxels in the axial scan was used as a parameter for tumor size. Prior to the DCE-MRI, T_2-weighted images were recorded by using a spin echo sequence with TR = 3000 ms and TE = 65 ms. The DCE-MRI was carried out by using an image matrix of 256×128, a field of view of 8×4 cm^2, and one excitation. Three proton density images (TR = 900 ms, TE = 3.2 ms, and $\alpha_{PD} = 20°$) and three T_1-weighted images were acquired before Gd-DTPA was administered, and T_1-weighted images were recorded for 15 min after the administration of Gd-DTPA. Gd-DTPA concentrations were calculated from signal intensities by using the method of Hittmair et al. [13]. The DCE-MRI series were analyzed on a voxel-by-voxel basis by using the arterial input function of Benjaminsen et al. [5] and the Tofts pharmacokinetic model [2]. Parametric images of K^{trans} and v_e were generated with the SigmaPlot software (SPSS Science, Chicago, IL, USA). For the V-27 tumors, median values of K^{trans} and v_e were calculated by excluding voxels in necrotic tissue (i.e. voxels with $v_e < 0.1$ or $v_e > 0.4$). The exclusion criteria were established as described in detail earlier [9]. For the CK-160 tumors, median values of K^{trans} and v_e were calculated from all tumor voxels because we have shown that the majority of the voxels in these tumors represent a chaotic mixture of parenchymal, connective, and necrotic tissue [14]. The strengths and limitations of our DCE-MRI procedure have been discussed thoroughly elsewhere [6,9].

Lymph node metastases

The mice were euthanized immediately after the DCE-MRI and examined for external lymph node metastases in the inguinal, axillary, interscapular, and submandibular regions and internal lymph node metastases in the abdomen and mediastinum. A dissecting microscope was used to detect enlarged lymph nodes. A lymph node was considered to be enlarged when the diameter was at least 1.3-fold longer than that of the corresponding lymph node in mice without tumors. Histological examination confirmed that enlarged lymph nodes showed metastatic growth. On the other hand, metastatic deposits could not be detected when selected normal-sized lymph nodes were examined histologically.

Statistical analysis

The Pearson product moment correlation test was used to search for correlations between parameters. Statistical comparisons of data were carried out by using the Student's t-test when the data complied with the conditions of normality and equal variance.

Under other conditions, comparisons were carried out by non-parametric analysis using the Mann-Whitney rank sum test. The Kolmogorov-Smirnov method was used to test for normality. Probability values of $p < 0.05$, determined from two-sided tests, were considered significant. The statistical analysis was carried out by using the SigmaStat statistical software (SPSS Science).

Results

The tumor transplantation site drained into the ipsilateral inguinal lymph nodes, and these lymph nodes constituted the principal site of metastatic growth. The draining lymphatics were enlarged in mice showing metastasis-positive inguinal lymph nodes. This is illustrated in Figure 1, which shows the draining lymphatics of a non-metastatic (Figure 1a) and a metastatic (Figure 1b) CK-160 tumor. In general, the draining lymphatics were larger in mice bearing metastatic V-27 tumors (Figure 1c) than in those bearing metastatic CK-160 tumors (Figure 1b).

Representative DCE-MRI data, uncorrected for necrosis, are presented in Figure 2, which shows the K^{trans} image, the K^{trans} frequency distribution, the v_e image, and the v_e frequency distribution of a non-metastatic CK-160 tumor (Figure 2a), a metastatic CK-160 tumor (Figure 2b), a non-metastatic V-27 tumor (Figure 2c), and a metastatic V-27 tumor (Figure 2d). The tumors of both lines were highly heterogeneous in K^{trans} with the highest values in the periphery and the lowest values in central regions. The intratumor heterogeneity in v_e was also substantial, but did not follow a fixed pattern in any of the lines (i.e. low and high values were seen in the center as well as in the periphery of the tumors).

K^{trans} and v_e did not correlate with tumor size in any of the lines. This is illustrated in Figure 3, which shows plots of median K^{trans} and median v_e versus tumor size for the CK-160 (Figure 3a) and the V-27 (Figure 3b) line. The K^{trans} and v_e values of the V-27 tumors in Figure 3b were corrected for necrosis.

Eight of the 21 CK-160 tumors gave rise to lymph node metastases. The metastatic growth in the metastasis-positive mice was limited to one or two lymph nodes. Median K^{trans} was higher in the non-metastatic than in the metastatic primary tumors ($p = 0.00033$; Figure 4a), whereas median v_e did not differ significantly between these two tumor groups ($p > 0.05$; Figure 4b). The metastatic and non-metastatic tumors did not differ significantly in size ($p > 0.05$; Figure 4c).

Thirty-two of the 35 mice bearing V-27 tumors developed lymph node metastases. In 12 mice, metastatic deposits were seen in inguinal lymph nodes only, whereas 20 mice showed metastatic growth in two or more sites. Median K^{trans} was higher in the poorly metastatic (0 or 1 positive lymph node) than in the highly metastatic (2 or more positive lymph nodes) primary tumors, whether the frequency distributions were corrected for necrosis ($p < 0.00001$; Figure 5a) or not ($p = 0.00003$; Figure 5b). Median v_e was higher in the poorly metastatic than in the highly metastatic tumors after the frequency distributions were corrected for necrosis ($p > 0.047$; Figure 5c), but not before the necrosis correction ($p > 0.05$; Figure 5d). The poorly and highly metastatic tumors did not differ significantly in size ($p > 0.05$; Figure 5e).

Discussion

Personalized cancer therapy requires adequate assays for identifying patients with particularly aggressive and treatment resistant tumors. The possibility that DCE-MRI may provide useful biomarkers of the potential of tumors to spread to regional lymph nodes was investigated in the present study of CK-160 cervical carcinoma and V-27 melanoma xenografts.

CK-160 and V-27 xenografts were chosen as model systems because a significant fraction of the

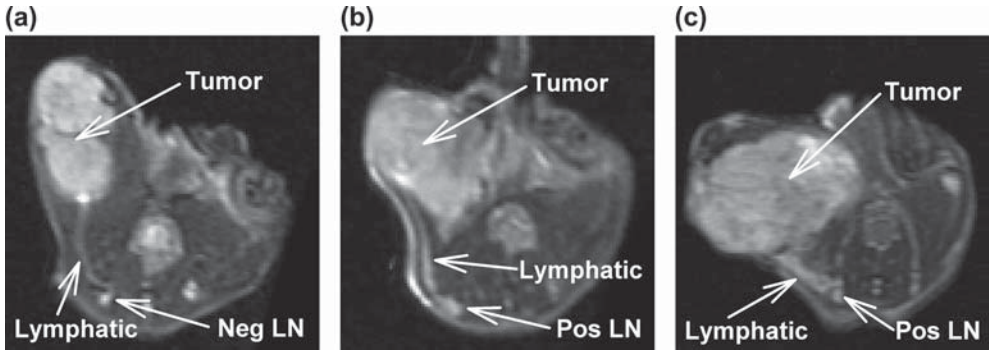

Figure 1. T_2-weighted MR-images showing the primary tumor, the draining lymphatic, and the ipsilateral inguinal lymph node of a mouse with a non-metastatic CK-160 tumor (a), a mouse with a metastatic CK-160 tumor (b), and a mouse with a metastatic V-27 tumor (c).

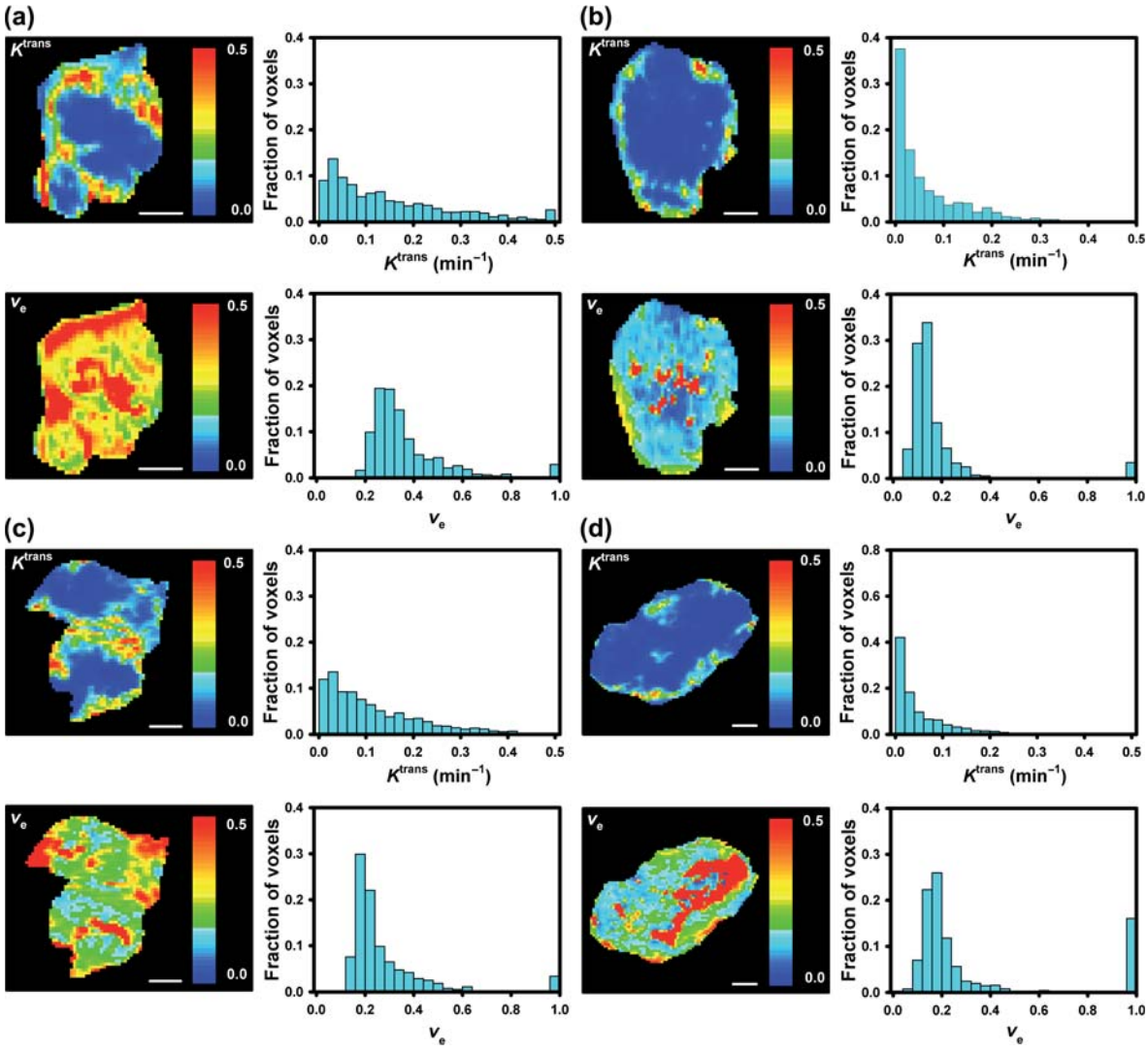

Figure 2. The K^{trans} image, K^{trans} frequency distribution, v_e image, and v_e frequency distribution of a non-metastatic CK-160 tumor (a), a metastatic CK-160 tumor (b), a non-metastatic V-27 tumor (c), and a metastatic V-27 tumor (d). Voxels in necrotic tissue have not been excluded from the images and frequency distributions. White scale bars: 3.0 mm.

tumors of these lines form lymph node metastases and the metastatic route is predictable when the tumors are transplanted intramuscularly. The intramuscular site is an ectopic site for cervical carcinoma as well as melanoma, and it has been suggested that ectopic tumors may be inferior to orthotopic tumors as experimental models for human cancer diseases [15]. Furthermore, the clinical relevance of experimental tumors initiated from long-term cultures of established cell lines has been questioned [16]. The cell cultures used in the present experiments were short-term cultures (i.e. the cells were obtained from our frozen stock shortly before transplantation), and we have shown previously that CK-160 and V-27 xenografted tumors initiated from short-term cultures have several biological properties in common with the donor patients' tumors [11,12]. These properties include histological appearance, response to treatment, aggressiveness, and metastatic pattern, suggesting that intramuscular CK-160 and V-27 xenografts should be adequate preclinical models for providing answers to the questions addressed in the present work.

A limitation of our study is that only a single axial slice through the tumor center was scanned. In two previous DCE-MRI studies of xenografted tumors in our laboratory, a slice-interleaving acquisition method was used to cover the tumors in full, and analysis of the data showed that the K^{trans} and v_e frequency distributions derived from the central axial scan were similar to those derived from the entire tumor [7,17]. It is thus unlikely that conclusions different from those reported here would have been obtained by scanning the entire tumor volume.

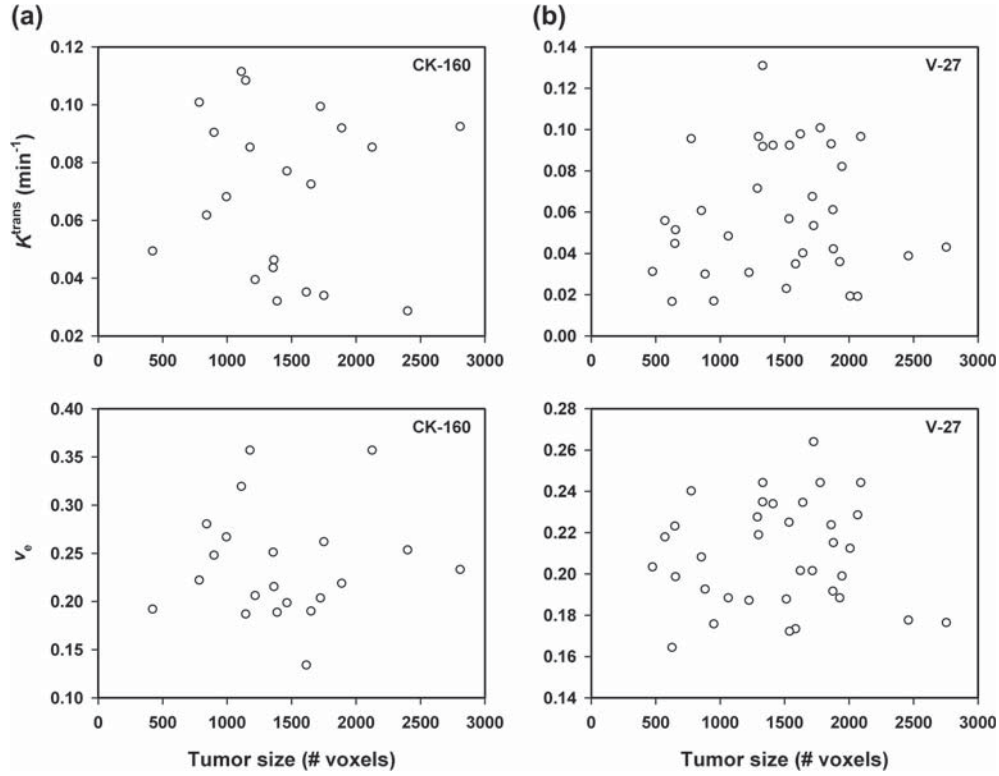

Figure 3. Median K^{trans} and median v_e versus tumor size for CK-160 (a) and V-27 (b) tumors. Voxels in necrotic tissue were excluded from the frequency distributions of the V-27 tumors before median values were calculated. Points represent single tumors.

Our study gives significant evidence that useful biomarkers for the metastatic potential of tumors may be provided by DCE-MRI. In the CK-160 line, the metastatic tumors showed lower K^{trans} values than the non-metastatic tumors, and in the V-27 line, the highly metastatic tumors showed lower K^{trans} values than the poorly metastatic tumors. Moreover, the v_e values were lower in the highly metastatic than in the poorly metastatic V-27 tumors.

The latter observation required that voxels in necrotic tissue were excluded from the v_e images. Moreover, necrosis-corrected K^{trans} images distinguished better between highly metastatic and poorly metastatic V-27 tumors than did uncorrected images. These observations emphasize the benefit of eliminating voxels in necrotic tissue from parametric DCE-MRI images of tumors. The exclusion criterion used here, however, may not be optimal in the clinical setting because v_e values are tumor dependent [18].

In previous investigations, we have demonstrated that V-27 tumors showing low K^{trans} values have high

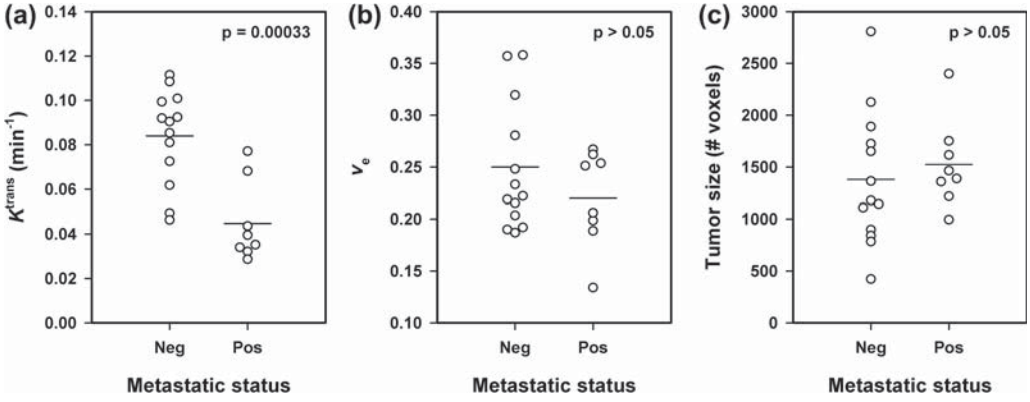

Figure 4. Median K^{trans} (a), median v_e (b), and size (c) of non-metastatic (Neg) and metastatic (Pos) CK-160 tumors. Points represent single tumors. Horizontal bars indicate mean values.

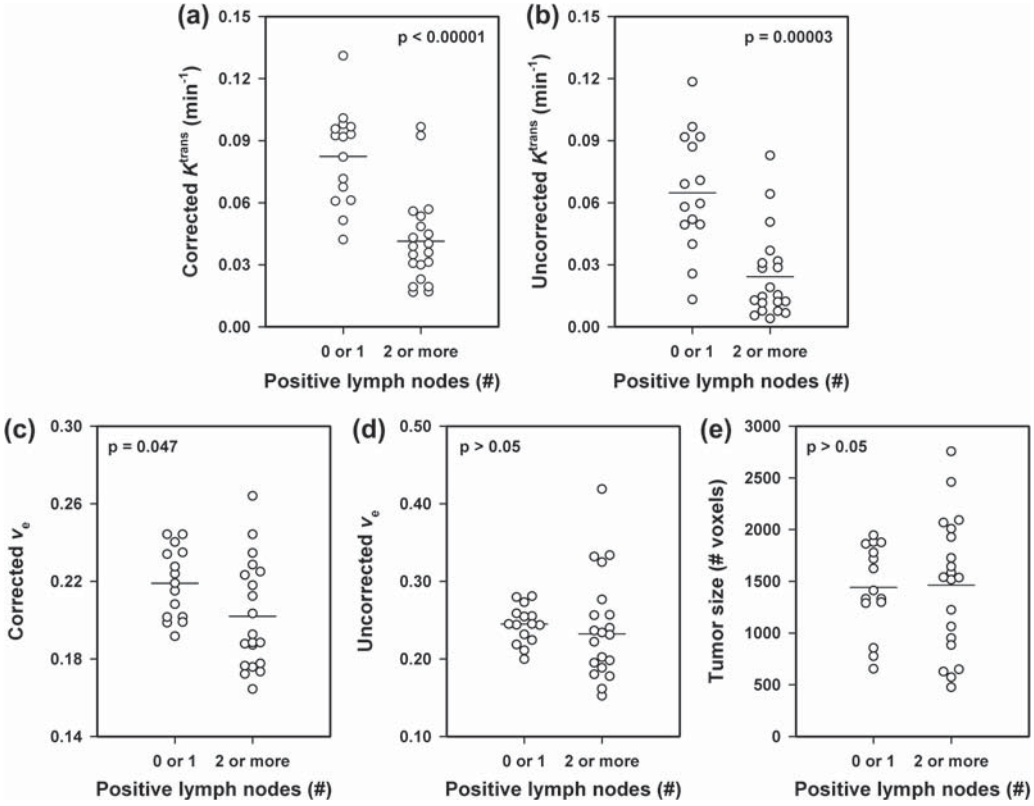

Figure 5. Necrosis-corrected median K^{trans} (a), uncorrected median K^{trans} (b), necrosis-corrected median v_e (c), uncorrected median v_e (d), and size (e) of poorly metastatic (0 or 1 positive lymph node) and highly metastatic (2 or more positive lymph nodes) V-27 tumors. Points represent single tumors. Horizontal bars indicate mean values.

fractions of hypoxic cells and that low K^{trans} values are associated with extensive hypoxia in CK-160 tumors [19,20]. It is thus likely that the associations between K^{trans} and metastatic propensity reported here reflect that the lymphogenous metastatic spread of CK-160 and V-27 xenografts is driven primarily by the extent of hypoxia in the primary tumor. This suggestion is consistent with the observation that tumor hypoxia may promote metastasis in several tumor types [10], including human and experimental cervical carcinomas [21–23] and melanoma xenografts [24]. Furthermore, we have shown previously that lymph node metastasis in CK-160 tumors is associated with the fraction of hypoxic cells in the primary tumor [25].

The lymphatics draining the tumor transplantation site were enlarged in the metastasis-positive mice, but not in the metastasis-negative mice. This observation suggests that tumor hypoxia promoted lymphogenous metastatic spread in CK-160 and V-27 tumors by up-regulating prolymphangiogenic factors, a suggestion that is in accordance with established mechanisms of lymph node metastasis. Thus, studies of several tumor types including cervical carcinoma have shown correlations between tumor hypoxia, the expression of the prolymphangiogenic factor vascular endothelial growth factor-C, lymphangiogenesis, and lymph node metastasis [26–28].

The observations reported here are in accordance with a study of Li et al. [29], who carried out experiments with xenografted tumors of two melanoma lines and showed that the K^{trans} for gadodiamide, a low-molecular-weight Gd-based contrast agent, was lower in the most metastatic line (C8161) than in the least metastatic line (A375P). The difference in K^{trans} between C8161 and A375P tumors was limited to the core of the tumors and was consistent with the histological observation that the density of functional blood vessels was higher in A375P than in C8161 tumors. However, only three C8161 tumors and four A375P tumors were imaged, and metastatic potential was based on historical data and not on the metastatic spread of the imaged tumors.

A non-invasive assay of the extent of hypoxia in tumors, hypoxia-induced resistance to radiation therapy, and hypoxia-induced metastatic dissemination would be useful for identifying cancer patients who might benefit from particularly aggressive treatment [10]. Several potentially useful MRI methods are being evaluated in preclinical studies, and most of these methods are based on the effects of the local oxygen concentration on the relaxation times

of ^{19}F or ^{1}H indicators, the magnetic susceptibility effects of oxy- and deoxyhemoglobin, or the effects of paramagnetic oxygen on the relaxation times of tissue water [30,31]. A DCE-MRI method with Gd-DTPA as contrast agent is particularly attractive because Gd-DTPA-based DCE-MRI is an established imaging method in clinical oncology. We have shown previously that low K^{trans} values and/or low v_e values are associated with extensive hypoxia in xenografted melanomas [7–9] and cervical carcinomas [20] and with poor radioresponsiveness [8,32] and hypoxia-induced pulmonary metastasis [33] in melanoma xenografts. In the present study, we showed that low values of K^{trans} and v_e are associated with high propensity for lymphogenous metastatic dissemination in both melanoma and cervical carcinoma xenografts. Taken together, our preclinical studies provide significant evidence that K^{trans} and v_e may be potentially useful biomarkers for hypoxia-induced tumor aggressiveness and suggest that patients with primary tumors characterized by low K^{trans} and low v_e values for Gd-DTPA may be attractive candidates for hypoxia-targeted treatments. It should be noted, however, that hypoxia-targeted treatments may not necessarily be effective in treating pre-existing metastases unless the metastases are severely hypoxic.

The potential of Gd-DTPA-based DCE-MRI as a non-invasive imaging method for identifying tumors that are particularly aggressive is currently being investigated in a large number of clinical studies. Our xenograft studies support the clinical attempts to establish DCE-MRI as a method for providing biomarkers for personalized cancer therapy and suggest criteria for identifying tumors that are likely to show hypoxia-induced aggressiveness. The validity of these criteria (i.e. low values of both K^{trans} and v_e) should be examined in prospective clinical investigations.

There is significant clinical evidence that hypoxia may promote malignant progression and metastatic dissemination in several histological types of cancer, including soft tissue sarcoma, prostate adenocarcinoma, colorectal carcinoma, carcinoma of the head and neck, and cervical carcinoma [10]. These tumor types are therefore interesting candidates for clinical investigations of DCE-MRI as a method for providing biomarkers for tumor aggressiveness. Such investigations should be designed to allow quantitative pharmacokinetic analysis of the DCE-MRI data and calculation of high-resolution parametric images of K^{trans} and v_e or parameters related to K^{trans} and v_e. Moreover, because pharmacokinetic models are not valid for necrotic tissue, criteria for excluding voxels in tumor necroses should be established.

Acknowledgements

Financial support was received from the Norwegian Cancer Society and the South-Eastern Norway Regional Health Authority. The authors report no conflicts of interest. The authors alone are responsible for the content and writing of the paper.

References

[1] Jennings D, Raghunand N, Gillies RJ. Imaging hemodynamics. Cancer Metastasis Rev 2008;27:589–613.
[2] Tofts PS, Brix G, Buckley DL, Evelhoch JL, Henderson E, Knopp MV, et al. Estimating kinetic parameters from dynamic contrast-enhanced T_1-weighted MRI of a diffusable tracer: Standardized quantities and symbols. J Magn Reson Imaging 1999;10:223–32.
[3] Zahra MA, Hollingsworth KG, Sala E, Lomas DJ, Tan LT. Dynamic contrast-enhanced MRI as a predictor of tumour response to radiotherapy. Lancet Oncol 2007;8:63–74.
[4] Hylton N. Dynamic contrast-enhanced magnetic resonance imaging as an imaging biomarker. J Clin Oncol 2006;24: 3293–8.
[5] Benjaminsen IC, Graff BA, Brurberg KG, Rofstad EK. Assessment of tumor blood perfusion by high-resolution dynamic contrast-enhanced MRI: A preclinical study of human melanoma xenografts. Magn Reson Med 2004;52: 269–76.
[6] Egeland TAM, Simonsen TG, Gaustad JV, Gulliksrud K, Ellingsen C, Rofstad EK. Dynamic contrast-enhanced magnetic resonance imaging of tumors: Preclinical validation of parametric images. Radiat Res 2009;172:339–47.
[7] Egeland TAM, Gaustad JV, Vestvik IK, Benjaminsen IC, Mathiesen B, Rofstad EK. Assessment of fraction of radiobiologically hypoxic cells in human melanoma xenografts by dynamic contrast-enhanced MRI. Magn Reson Med 2006;55:874–82.
[8] Gulliksrud K, Øvrebø KM, Mathiesen B, Rofstad EK. Differentiation between hypoxic and non-hypoxic experimental tumors by dynamic contrast-enhanced magnetic resonance imaging. Radiother Oncol 2011;98:360–4.
[9] Egeland TAM, Gulliksrud K, Gaustad JV, Mathiesen B, Rofstad EK. Dynamic contrast-enhanced MRI of tumor hypoxia. Magn Reson Med 2012;67:519–30.
[10] Vaupel P, Mayer A. Hypoxia in cancer: Significance and impact on clinical outcome. Cancer Metastasis Rev 2007; 26:225–39.
[11] Ellingsen C, Natvig I, Gaustad JV, Gulliksrud K, Egeland TAM, Rofstad EK. Human cervical carcinoma xenograft models for studies of the physiological microenvironment of tumors. J Cancer Res Clin Oncol 2009;135:1177–84.
[12] Rofstad EK, Mathiesen B. Metastasis in melanoma xenografts is associated with tumor microvascular density rather than extent of hypoxia. Neoplasia 2010;12:889–98.
[13] Hittmair K, Gomiscek G, Langenberger K, Recht M, Imhof H, Kramer J. Method for the quantitative assessment of contrast agent uptake in dynamic contrast-enhanced MRI. Magn Reson Med 1994;31:567–71.
[14] Ellingsen C, Egeland TAM, Galappathi K, Rofstad EK. Dynamic contrast-enhanced magnetic resonance imaging of human cervical carcinoma xenografts: Pharmacokinetic analysis and correlation to tumor histomorphology. Radiother Oncol 2010;97:217–24.
[15] Killion JJ, Radinsky R, Fidler IJ. Orthotopic models are necessary to predict therapy of transplantable tumors in mice. Cancer Metastasis Rev 1999;17:279–84.

[16] Talmadge JE, Singh RK, Fidler IJ, Raz A. Murine models to evaluate novel and conventional therapeutic strategies for cancer. Am J Pathol 2007;170:793–804.

[17] Gaustad JV, Benjaminsen IC, Graff BA, Brurberg KG, Ruud EBM, Rofstad EK. Intratumor heterogeneity in blood perfusion in orthotopic human melanoma xenografts assessed by dynamic contrast-enhanced magnetic resonance imaging. J Magn Reson Imaging 2005;21:792–800.

[18] Egeland TAM, Gaustad JV, Galappathi K, Rofstad EK. Magnetic resonance imaging of tumor necrosis. Acta Oncol 2011;50:427–34.

[19] Øvrebø KM, Hompland T, Mathiesen B, Rofstad EK. Assessment of hypoxia and radiation response in intramuscular experimental tumors by dynamic contrast-enhanced magnetic resonance imaging. Radiother Oncol 2012;102: 429–35.

[20] Ellingsen C, Egeland TAM, Gulliksrud K, Gaustad JV, Mathiesen B, Rofstad EK. Assessment of hypoxia in human cervical carcinoma xenografts by dynamic contrast-enhanced magnetic resonance imaging. Int J Radiat Oncol Biol Phys 2009;73:838–45.

[21] Sundfør K, Lyng H, Rofstad EK. Tumour hypoxia and vascular density as predictors of metastasis in squamous cell carcinoma of the uterine cervix. Br J Cancer 1998; 78:822–7.

[22] Pitson G, Fyles A, Milosevic M, Wylie J, Pintilie M, Hill RP. Tumor size and oxygenation are independent predictors of nodal disease in patients with cervix cancer. Int J Radiat Oncol Biol Phys 2001;51:699–703.

[23] Cairns RA, Hill RP. Acute hypoxia enhances spontaneous lymph node metastasis in an orthotopic murine model of human cervical carcinoma. Cancer Res 2004;64: 2054–61.

[24] Rofstad EK, Rasmussen H, Galappathi K, Mathiesen B, Nilsen K, Graff BA. Hypoxia promotes lymph node metastasis in human melanoma xenografts by up-regulating the urokinase-type plasminogen activator receptor. Cancer Res 2002;62:1847–53.

[25] Ellingsen C, Hompland T, Mathiesen B, Rofstad EK. Microenvironment-associated lymph node metastasis of human cervical carcinoma xenografts. Acta Oncol 2012;51: 465–72.

[26] Schoppmann SF, Fenzl A, Schindl M, Bachleitner-Hofmann T, Nagy K, Gnant M, et al. Hypoxia inducible factor-1α correlates with VEGF-C expression and lymphangiogenesis in breast cancer. Breast Cancer Res Treat 2006; 99:135–41.

[27] Min Y, Ghose S, Boelte K, Li J, Yang L, Lin PC. C/EBP-δ regulates VEGF-C autocrine signaling in lymphangiogenesis and metastasis of lung cancer through HIF-1α. Oncogene 2011;30:4901–9.

[28] Chaudary N, Milosevic M, Hill RP. Suppression of vascular endothelial growth factor receptor 3 (VEGFR3) and vascular endothelial growth factor C (VEGFC) inhibits hypoxia-induced lymph node metastases in cervix cancer. Gynecol Oncol 2011;123:393–400.

[29] Li LZ, Zhou R, Xu HN, Moon L, Zhong T, Kim EJ, et al. Quantitative magnetic resonance and optical imaging biomarkers of melanoma metastatic potential. Proc Natl Acad Sci USA 2009;106:6608–13.

[30] Tatum JL, Kelloff GJ, Gillies RJ, Arbeit JM, Brown JM, Chao KS, et al. Hypoxia: Importance in tumor biology, noninvasive measurement by imaging, and value of its measurement in the management of cancer therapy. Int J Radiat Biol 2006;82:699–757.

[31] Pacheco-Torres J, López-Larrubia P, Ballesteros P, Cerdán S. Imaging tumor hypoxia by magnetic resonance methods. NMR Biomed 2011;24:1–16.

[32] Øvrebø KM, Gulliksrud K, Mathiesen B, Rofstad EK. Assessment of tumor radioresponsiveness and metastatic potential by dynamic contrast-enhanced magnetic resonance imaging. Int J Radiat Oncol Biol Phys 2011;81:255–61.

[33] Øvrebø KM, Ellingsen C, Galappathi K, Rofstad EK. Dynamic contrast-enhanced magnetic resonance imaging of the metastatic potential of melanoma xenografts. Int J Radiat Oncol Biol Phys 2012;83:e121–7.